

The PIR domain of Grb14 is an intrinsically unstructured protein: implication in insulin signaling

Karine Moncoq^{a,1}, Isabelle Broutin^{a,1,*}, Valéry Larue^a, Dominique Perdereau^b,
Katia Cailliau^c, Edith Browaeys-Poly^c, Anne-Françoise Burnol^b, Arnaud Ducruix^a

^aLaboratoire de Cristallographie et RMN Biologiques, Faculté de Pharmacie Paris 5, 4 avenue de l'Observatoire, 75270 Paris Cedex 06, France

^bInstitut Cochin INSERM U567, CNRS UMR 8104, Département d'Endocrinologie, 24 rue du Faubourg Saint-Jacques, 75674 Paris, France

^cUniversité des Sciences et Technologies de Lille, Laboratoire de Biologie du Développement, UE 1033, Bâtiment SN3, Villeneuve d'Ascq Cedex, France

Received 11 July 2003; revised 22 September 2003; accepted 22 September 2003

First published online 22 October 2003

Edited by Thomas L. James

Abstract Grb14 belongs to the Grb7 family of adapter proteins and was identified as a negative regulator of insulin signal transduction. Its inhibitory effect on the insulin receptor kinase activity is controlled by a newly discovered domain called PIR. To investigate the biochemical and biophysical characteristics of this new domain, we cloned and purified recombinant PIR-SH2, PIR, and SH2 domains. The isolated PIR and PIR-SH2 domains were physiologically active and inhibited insulin-induced reinitiation of meiosis in the *Xenopus* oocytes system. However, NMR experiments on ¹⁵N-labelled PIR revealed that it did not present secondary structure. These results suggest that the PIR domain belongs to the growing family of intrinsically unstructured proteins.

© 2003 Federation of European Biochemical Societies. Published by Elsevier B.V. All rights reserved.

Key words: Grb7 family; Phosphorylated insulin receptor interacting region; Signal transduction; Unstructured protein

1. Introduction

Molecular adapters are involved in multiple protein/protein and protein/phospholipid interactions required in cascade activation. This makes them essential components of signal transduction pathways.

A new family of adapters has recently emerged, the Grb7 family composed of Grb7, Grb10 and Grb14 [1]. All members of this family are characterized by several conserved domains: an N-terminal proline rich region, a Ras-associated-like domain, a pleckstrin homology (PH) domain, and a C-terminal Src homology 2 (SH2) domain. Like other adapter molecules, Grb7 family members have been shown to interact with a variety of cell surface receptors and also with other signaling

proteins. Most of these interactions are mediated by their SH2 domain in a phosphotyrosine-dependent manner [2].

To date, limited information is available concerning the biological roles of Grb7, Grb10 and Grb14.

- Various studies have suggested the importance of Grb7 in tumor progression [3,4] and in the regulation of cell migration [5,6].
- Grb10 can be found as six different isoforms, whose functions are not yet fully elucidated. Grb10 can bind to Raf and MEK, and thus is likely to be implicated in the MAP Kinase cascade and in cell proliferation [7].
- Grb14 is the most recently identified member of the Grb7 family of adapters. It is specifically expressed in insulin-sensitive tissues. Furthermore, insulin induces Grb14 binding to the insulin receptor (IR) in vivo in rat liver, suggesting that it is a physiological insulin signaling effector [8]. Overexpression of Grb14 in CHO-IR cells inhibits insulin-stimulated DNA and glycogen synthesis or tyrosine phosphorylation of proteins [8,9].

In vitro tyrosine kinase assays have shown that the Grb7 family members inhibit the IR catalytic activity, and that Grb14 is the most potent inhibitor [10,11]. For all three Grbs, the inhibitory action on the IR kinase activity is mediated by a new interaction domain located between the SH2 and PH domains called either BPS (between PH and SH2) [12] or PIR (phosphorylated insulin receptor interacting region) [8,13]. PIR specifically binds to the regulatory kinase loop of the IR. This domain is highly conserved among the members of the Grb7 family and does not show any similarity with any other known protein interaction domain. To date, only one other partner of the PIR domain has been described, the protein kinase C ζ interacting protein (ZIP) [14].

The three Grbs members are all able to bind to the activated IR through both their PIR and SH2 domains, but interestingly, the relative importance of the two domains depends on the member of the Grb7 family and the receptor tyrosine kinase considered. For Grb10, the PIR and SH2 domains interact equally with the IR, while PIR seems to be the major binding domain with the insulin-like growth factor receptor (IGF-R) [12,15,16]. By contrast, the SH2 domain of Grb7 is sufficient for the interaction with IR [13]. In the case of Grb14, the interaction with IR is mainly due to the PIR domain [8,11]. Therefore the differential binding of PIR and SH2 domains should be a determinant for the specificity in Grbs' interactions with receptor tyrosine kinase.

*Corresponding author. Fax: (33)-1-53 73 99 25.

E-mail address: broutin@pharmacie.univ-paris5.fr (I. Broutin).

¹ These authors contributed equally to this work.

Abbreviations: BPS, between PH and SH2; DTT, dithiothreitol; GVBD, germinal vesicle breakdown; HSQC, heteronuclear single quantum correlation; IGF-R, insulin-like growth factor receptor; IR, insulin receptor; IUP, intrinsically unstructured protein; PH, pleckstrin homology; PIR, phosphorylated insulin receptor interacting region; PKC ζ , protein kinase C ζ ; SH2, Src homology 2; ZIP, protein kinase C ζ interacting protein

SH2 domains have been studied extensively; over a hundred structures exist in the PDB [17]. However, until now there is no structural data for the PIR domain. This study is the first biophysical analysis of the PIR domain. Using heteronuclear NMR spectroscopy we describe the unstructured nature of PIR. *Xenopus* oocytes have been used as an experimental model for activity analysis of recombinant PIR domain. In spite of the lack of ordered structure, PIR is physiologically active. Taken together, these results suggest that PIR belongs to the expanding family of intrinsically unstructured proteins (IUPs).

2. Materials and methods

2.1. Cloning and expression of recombinant PIR and PIR-SH2 domains of Grb14

Constructs for the PIR (encoding residues 361–435), PIR-SH2 (encoding residues 361–538) and SH2 (encoding residues 430–538) domains of Grb14 were subcloned into expression vector pET28b (Novagen). All constructs were verified by DNA sequencing. *Escherichia coli* strain BL21-DE3 was transformed with plasmids and cultures were grown in Luria broth with 30 $\mu\text{g ml}^{-1}$ kanamycin (Sigma) at 37°C to an $\text{OD}_{600\text{nm}}$ of 1.0 for the PIR and PIR-SH2 domains, and to 0.6 for the SH2 domain. Protein expression was induced by addition of 0.1 mM final IPTG (Sigma) for 4 h at 28°C. Cells were harvested by centrifugation at $8000 \times g$ for 30 min and immediately frozen at -80°C .

2.2. Purification and NMR sample preparation

2.2.1. Purification of recombinant PIR-SH2 domain of Grb14. All purification procedures were carried out at 4°C. Cells (9 g) were suspended in 60 ml of 50 mM Tris-HCl buffer pH 8.8 containing 500 mM NaCl, 1% (v/v) Triton X-100, 1 mM phenylmethylsulfonyl fluoride (PMSF), 1 mM dithiothreitol (DTT), and were disrupted by sonication. CaCl_2 to a final concentration of 0.6 mM was added to remove DNA, followed by centrifugation at $8000 \times g$. The supernatant was dialyzed against a 50 mM Tris-HCl buffer pH 8.0 containing 500 mM NaCl, 0.1% (v/v) Triton X-100, 1 mM DTT and 5 mM EDTA to remove CaCl_2 , and then against a 50 mM Tris-HCl buffer pH 8.0 with 1 mM DTT (buffer A). The dialyzed supernatant was loaded onto a Sepharose high performance Q column (Pharmacia Biotech) equilibrated with buffer A. The flow-through fractions were recovered and applied onto a Sepharose high performance SP column (Pharmacia Biotech) equilibrated with buffer A. Proteins were eluted with a linear gradient (0–0.2 M) of NaCl in buffer A (total volume 180 ml) at a flow rate of 1 ml min^{-1} . The resulting fractions were chromatographed on a gel-filtration column (Sephacryl S-100, Pharmacia Biotech) equilibrated with a 50 mM succinate buffer pH 6.5 containing 150 mM NaCl and 1 mM DTT at a flow rate of 0.3 ml min^{-1} . The PIR-SH2 fractions were concentrated to about 10 mg ml^{-1} (0.5 mM) and stored at -80°C .

2.2.2. Purification of recombinant PIR domain of Grb14. Cells (5 g) were suspended in 20 ml of 50 mM glycine buffer pH 9.5 containing 500 mM NaCl, 1% (v/v) Triton X-100, 1 mM PMSF, 1 mM DTT, and were disrupted by sonication. CaCl_2 to a final concentration of 0.6 mM was added to remove DNA followed by centrifugation at $8000 \times g$. The supernatant was dialyzed against a 50 mM glycine buffer pH 9.5 containing 500 mM NaCl, 0.1% (v/v) Triton X-100, 5 mM EDTA to remove CaCl_2 , and then against a 50 mM Tris-HCl buffer pH 8.0 with 50 mM NaCl, 0.1% (v/v) Triton X-100, 5 mM EDTA. The dialyzed supernatant was diluted three-fold in 50 mM Tris-HCl buffer pH 8.0 (buffer A) and applied onto a cation exchange high performance SP column (Pharmacia Biotech). Proteins were eluted with a linear gradient (0–0.35 M) of NaCl in buffer A (total volume 140 ml). PIR fractions were further purified on a gel-filtration column (Sephacryl S-100, Pharmacia Biotech) equilibrated with buffer A at a flow rate of 0.5 ml min^{-1} . PIR was stored at 4°C at about 5 mg ml^{-1} in 50 mM Tris-HCl pH 8.0, 1 mM TCEP (Tris-(2-carboxyethyl)phosphine).

2.2.3. Purification of recombinant SH2 domain of Grb14. Cells (4 g) were suspended in 20 ml of 50 mM Tris-HCl buffer pH 8.5 containing 500 mM NaCl, 0.1% (v/v) Triton X-100, 1 mM PMSF, 5 mM EDTA, 5 mM DTT, and were disrupted by sonication. Cells debris were

pelleted and the supernatant was diluted to a final volume of 200 ml in 50 mM Tris-HCl buffer pH 8.0 with 1 mM DTT (buffer A) before being loaded onto a Sepharose high performance Q column (Pharmacia Biotech) equilibrated with buffer A. Proteins were eluted with a linear gradient (0.05–0.150 M) of NaCl in buffer A (total volume 180 ml) at a flow rate of 1 ml min^{-1} . The resulting fractions were chromatographed on a gel-filtration column (Sephacryl S-100, Pharmacia Biotech) equilibrated with a 50 mM Tris-HCl buffer pH 8.5 containing 100 mM NaCl and 1 mM DTT at flow rate of 0.3 ml min^{-1} . The yield was 20 mg per liter of culture. The SH2 fractions were concentrated to about 10 mg ml^{-1} (0.5 mM) and stored at -80°C .

Every step of purification was verified by sodium dodecyl sulfate–polyacrylamide gel electrophoresis (SDS–PAGE) according to the Laemmli method.

Proteins concentrations were determined using calculated extinction coefficients. Proteins were characterized using N-terminal sequence determination.

For NMR experiments, ^{15}N -labelled PIR and PIR-SH2 samples were obtained by growing the corresponding strains in Martek-9N medium (Martek Inc.) containing 30 $\mu\text{g ml}^{-1}$ of kanamycin and supplemented with 2 g l^{-1} of ^{15}N -celtane. The labelled proteins were purified as described above, and concentrated at about 0.5 mM in 50 mM potassium phosphate buffer pH 7.0 containing 10% D_2O . The yield of production of the ^{15}N -labelled proteins was the same as for the unlabelled ones, i.e. 15 mg of pure PIR-SH2 and 5 mg of pure PIR for 1 l ^{15}N -labelled medium.

2.3. NMR experiments

NMR samples were prepared in $\text{H}_2\text{O}/^2\text{H}_2\text{O}$ (90/10). The ^{15}N -labelled PIR concentration was circa 1 mM (pH 5.0). 1D, 2D and 3D experiments were recorded at 300 K on a Bruker 600 MHz Avance spectrophotometer equipped with a triple resonance inverse probe. 2D homonuclear NOESY and TOCSY were recorded with the identical spectral width of 7800 Hz in both dimensions, using mixing times of 200 and 55 ms, respectively. A 2D ^{15}N – ^1H echo/antiecho heteronuclear single quantum correlation (HSQC) [18,19] was recorded with spectral widths of 3000 Hz and 1580 Hz in the ^1H and ^{15}N dimensions, respectively. 3D NOESY-HSQC [20] and 3D TOCSY-HSQC [21] were recorded with spectral widths of 4800, 2400, 8400 Hz, respectively for amide ^1H , ^{15}N and ^1H dimensions, and mixing times of 200 ms (NOESY) and 55 ms (TOCSY). Heteronuclear ^{15}N – ^1H NOE cross-relaxation rates were measured [22,23]. Two refocused reverse 2D INEPT spectra were recorded in an interleaved manner, either with or without proton saturation during the relaxation delay (4 s) prior to the starting 90 ^{15}N pulse. Apart from the proton saturation, all other parameters were identical in both experiments. Data processing was done with FELIX (MSI, San Diego, CA, USA).

2.4. *Xenopus* oocyte studies

After anesthesia with MS 222 (1 g l^{-1} , Sandoz), *Xenopus laevis* ovarian lobes were surgically removed and placed in modified OR2 medium, lacking potassium (82.5 mM NaCl, 1 mM MgCl_2 , 1 mM CaCl_2 , 1 mM Na_2HPO_4 , 5 mM HEPES, adjusted to pH 7.4), supplemented with streptomycin/penicillin (50 $\mu\text{g ml}^{-1}$, Eurobio), tetracycline (50 $\mu\text{g ml}^{-1}$, Sigma), sodium pyruvate (225 $\mu\text{g ml}^{-1}$, Sigma) and soybean trypsin inhibitor (30 $\mu\text{g ml}^{-1}$, Sigma). Full grown stage VI *X. laevis* oocytes were obtained by defolliculation using a 1 h treatment with collagenase A (1 mg ml^{-1} , Boehringer Mannheim) and achieved by manual dissection. Oocytes were kept at 19°C in modified OR2 medium. Oocytes were treated with insulin 1 μM . Microinjections of PIR, PIR-SH2 and SH2 domains were processed in the equatorial region 1 h before insulin stimulation. Controls were performed without protein injection before insulin stimulation. Germinal vesicle breakdown (GVBD) was determined by the appearance of a white spot at the center of the animal pole 20 h after insulin treatment. For each injection the experiment was performed on at least two different batches of 20 oocytes each.

3. Results

3.1. Production of the recombinant proteins

To study the binding and inhibitory properties of the Grb14 protein, its PIR, PIR-SH2 and SH2 domains were overex-

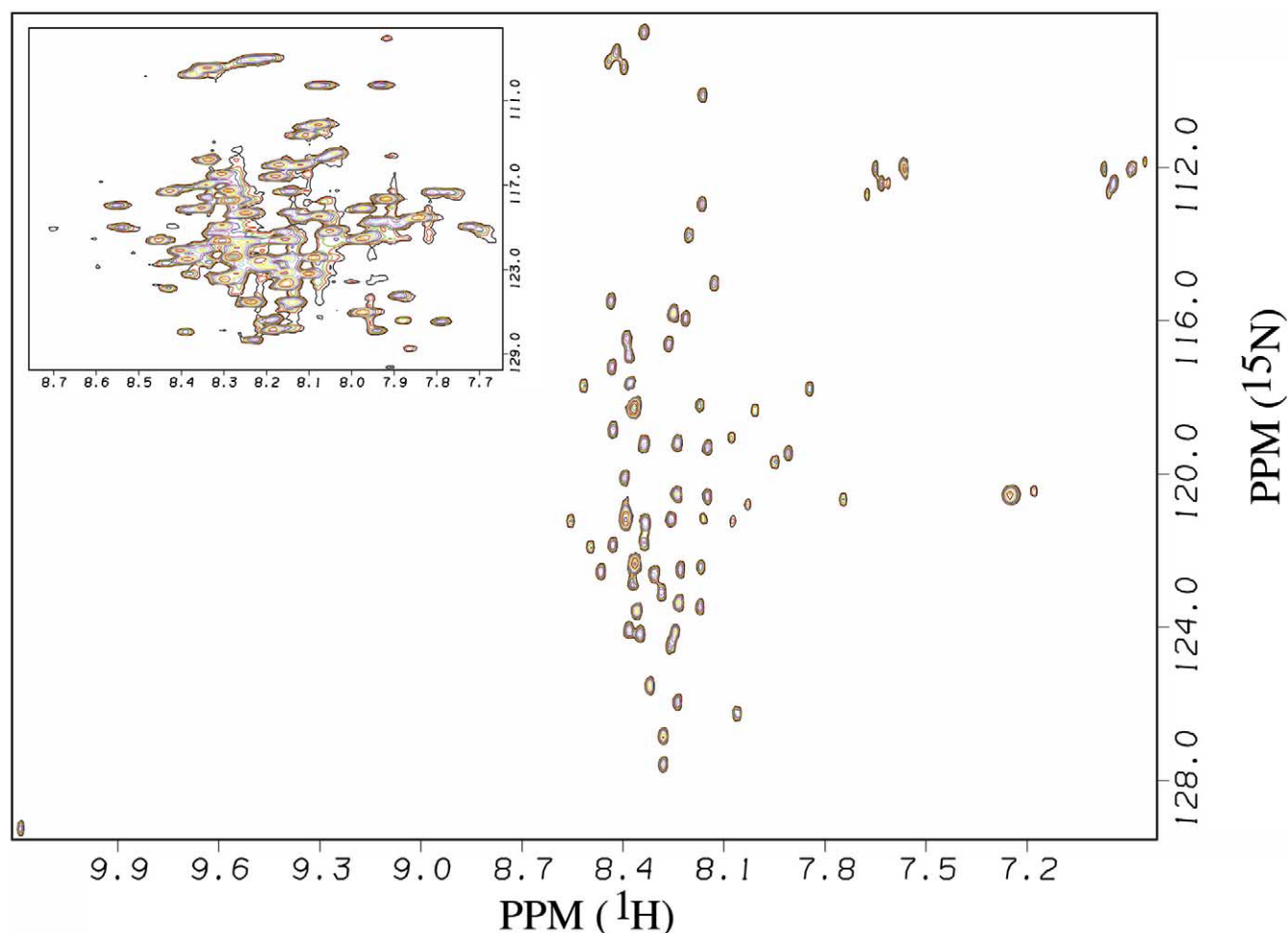


Fig. 1. ^1H – ^{15}N HSQC spectra of the ^{15}N -labelled PIR protein. The inset corresponds to a different level of signal cutoff for direct comparison with Fig. 2.

pressed and purified. Several constructs using fusions or tags were tested but they all led to either unexpressed or insoluble proteins. Consequently, all three domains were expressed in their native forms. The HCA (hydrophobic cluster analysis) program [24] and sequence alignment analysis were used to optimize selection of the domains. Subsequently the recombinant proteins expressed in *E. coli* were soluble.

Some purification problems were encountered with the PIR and PIR-SH2 domains, as PIR is extremely basic (pI 9.86) causing unspecific binding with DNA. To overcome this difficulty, precipitation of DNA by CaCl_2 (T. Rabilloux, personal communication) was performed, allowing the purification of PIR and PIR-SH2 in only two steps with a yield of 4.5 and 15 mg, respectively, of pure protein per liter of culture.

This study is the first successful report of PIR purification [10].

3.2. NMR experiments

The structure of PIR was investigated by solution NMR. In a preliminary NMR study, a 1D experiment was recorded (data not shown). The 1D spectra showed poor dispersion of the aliphatic and amide signals, and absence of high field shifted methyl groups. In a 2D ^{15}N – ^1H HSQC experiment (Fig. 1), although about 70 amide cross-peaks were observed out of the 74 expected, the very narrow spread of the reso-

nance frequencies for amide protons in both ^{15}N and ^1H dimensions is typical of a largely unfolded protein [25]. The absence of secondary structure in solution is confirmed by the absence of cross-peaks in the NH–NH region of a 2D NOESY experiment and by the absence of high-field shifted methyl groups (data not shown). They all cluster around random-coil shifts at 0.92 ppm. Moreover, in a NOESY-HSQC 3D experiment, no cross-peaks were observed in the NH–NH region except for two peaks at frequencies of 8.36 ppm/8.01 ppm and 8.22 ppm/7.90 ppm. Consequently, no sequential attribution was performed due to superimposition, poor dispersion of the $\text{H}\alpha$ and $\text{H}\beta$ chemical shift and the absence of sequential or long-distance cross-peaks in 2D and 3D experiments. Taken together, these results strongly suggest that the PIR domain is largely unstructured in solution [26,27].

To further investigate the conformational state of the PIR domain, we measured the heteronuclear ^{15}N – ^1H NOE effects. Heteronuclear ^{15}N – ^1H Overhauser enhancements ranged from -4.93 to -0.12 and were modulated by molecular motions: ^{15}N – ^1H NOEs decreased as the correlation time increased. These values can thus be used to distinguish rigid from mobile sites within a protein [22,28]. All heteronuclear NOEs were negative, ranging from -1 to -3 , except for five peaks which had higher values ranging from -0.6 to -0.8 (Fig. 2). These NOE values for 93–95% of the PIR amino acid chain corre-

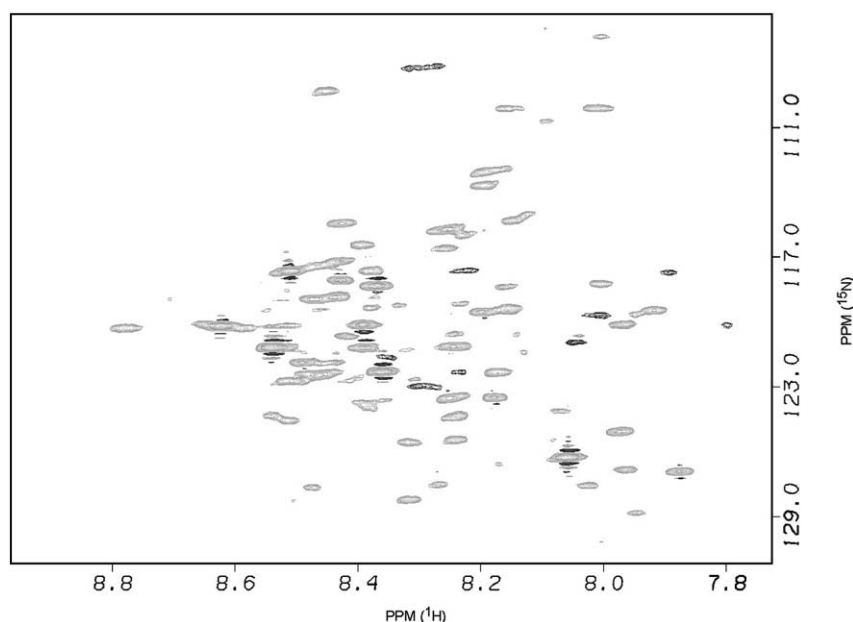


Fig. 2. Backbone dynamic of the PIR Grb14 domain. Heteronuclear ^{15}N - ^1H NOEs spectra of the ^{15}N -labelled PIR protein recorded at 600 MHz and 300 K. In gray are represented NOE effects between -1 and -3 , which correspond to an estimated overall correlation time of 0.1 ns. In black are represented NOE effects between -0.6 and -1 , which correspond to an estimated overall correlation time of 1 ns. A qualitative analysis of the spectra shows that 5–7% of the PIR domain is less mobile than the rest of the protein.

spond to movements on the 0.1 ns time scale, which is typical of an unstructured protein and confirms the other NMR results. Only 5–7% of the amino acids of the PIR protein exhibited slower movement (1 ns time scale). Because disordered proteins usually acquire folded structure when in complex with other proteins, this could indicate a nucleation point for PIR folding.

3.3. *In vivo* functional studies in *X. laevis* oocytes

In order to determine whether PIR was biologically active or not *in vivo* despite its lack of structure, we have used *X. laevis* oocytes, physiologically arrested at the G2 stage of the first meiotic prophase, as a model system. The natural inducer progesterone [29] and some growth factors (IGF-1, insulin and EGF) [30,31] were used to reinitiate the oocyte cycle and induce entry into the M phase, thus triggering a GVBD. *Xenopus* oocytes react as an all or none system after activation.

Microinjection of PIR, heated PIR, PIR-SH2, or SH2 domains was processed 1 h prior to insulin stimulation. The results are summarized in Fig. 3. The injection of 12.5 ng of PIR-SH2 (0.6 pmol) was sufficient to inhibit insulin-induced GVBD. For the PIR domain, microinjection of 39 ng totally blocks the GVBD. However the microinjection of 26 ng of PIR partly blocks the GVBD. This suggests that the minimal amount of PIR Grb14 needed to suppress insulin-induced GVBD is close to 30 ng (3.75 pmol). Those amounts are physiologically relevant. The SH2 domain alone had no effect on oocyte maturation even when injected in excess.

This indicates that the PIR domain is physiologically active *in vivo* despite its lack of structure, and implies that PIR belongs to the new family of IUPs [32], also called 'natively unfolded proteins'. As heat stability is one characteristic of this family of proteins, PIR was heated to 90°C for 30 min and microinjected in oocytes. The heat-treated PIR blocked equally well as the untreated PIR insulin-induced oocyte mat-

uration. The ability of PIR to retain its inhibitory activity following extreme heat treatment is consistent with its classification as an IUP.

4. Discussion

The findings described here constitute the first detailed structural and biochemical analyses of the new domain PIR of Grb14. Here, PIR was expressed and purified in sufficient quantities for structural studies. Firstly, we have demonstrated that PIR domain is unstructured in solution as shown by heteronuclear NMR. This type of NMR experiment is considered the most versatile and powerful tool to study proteins disorder. Secondly, recombinant PIR and PIR-SH2 do-

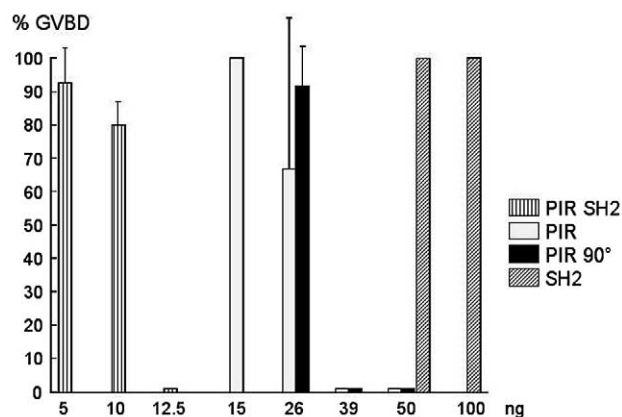


Fig. 3. Effect of the injection of PIR-SH2, PIR and SH2 proteins on insulin-induced oocyte maturation. Oocytes were microinjected with increasing amounts of PIR-SH2, PIR, heat-denatured PIR (90°C), and SH2 proteins as indicated. Oocyte maturation was assessed by GVBD detection. Results are expressed as the percentage of GVBD, and are the mean \pm S.E.M. of two to three independent experiments.

mains were shown to be physiologically active in the *in vivo* model system *Xenopus* oocytes. These results strongly suggest an unstructured functional state of the PIR domain, leading us to classify it as a new member of the family of IUPs.

IUPs belong to a class of proteins that exhibits little secondary structure, high flexibility, and low compactness [33–35]. Consequently, unstructured proteins are characterized by proteolytic sensitivity and heat stability. We have shown that heat-treated PIR does not become insoluble and it retains its ability to inhibit the insulin-induced maturation of oocytes. The central sequence of PIR is extremely hydrophilic which is energetically favorable for unstructured proteins. Consistent with these characteristics, the SH2 domain of Grb10 has been purified from the recombinant PIR-SH2 domains using protease [10], indicating the proteolytic sensitivity of PIR. In the last 10 years, the number of proteins shown to contain natively unfolded domain(s) under physiological conditions has increased exponentially. This is mainly due to the development of structural genomics. Of all the purified open reading frames, around 8% are shown to be unfolded (A. Poupon, personal communication). Furthermore, ‘natively unfolded proteins’ are observed to be key regulatory checkpoints of several signal transduction pathways [34,36]. It has been suggested that the absence of rigid globular structure under physiological conditions might represent a considerable functional advantage. The large flexibility of natively unfolded proteins allows them to interact efficiently with several different targets [32,34].

The PIR partners described so far are the IR and a new

downstream partner of Grb14, ZIP [14]. A model has been proposed for the role of ZIP in the Grb14 pathway. ZIP could act as a functional scaffold protein connecting protein kinase C ζ (PKC ζ) to Grb14. ZIP interacts with the V1 domain of PKC ζ through its AID domain and with the PIR of Grb14 through its ZZ zinc finger domain [14]. Upon insulin stimulation, PIR binds to the activated IR regulatory kinase loop. PIR phosphorylation by PKC ζ via ZIP leads to an increased Grb14 inhibitory action on IR [14]. The interaction between PIR and ZIP does not alter the insulin-induced Grb14-IR interaction. The ability of PIR to bind to diverse ligands such as the tyrosine kinase loop and ZZ zinc finger requires a structural flexibility which is consistent with a ‘natively unfolded’ domain. Nevertheless, unstructured proteins may undergo some degree of folding upon binding to their partner [37], a process termed ‘induced folding’. PIR probably acquires structure when complexed with binding partners in its cellular context as suggested by the $^{15}\text{N}\{^1\text{H}\}$ -NOE experiment.

However the target of the Grb7 family of proteins remains to be elucidated. All three PIR-SH2 domains of the Grb7 family of proteins interact with IR phosphorylated regulatory kinase loop consisting of residues $^{1150}\text{DFGMTRDIP-YETDpYpYRKGGKGLLP}^{1172}$. Structures of active and inactive state of IR have both been resolved by crystallography [38,39]. In the inactive state, this loop is not phosphorylated and IR is autoinhibited by the binding of tyrosine 1162 with the catalytic site. In the active state, when the three tyrosines 1158 1162 and 1163, are phosphorylated, the kinase loop

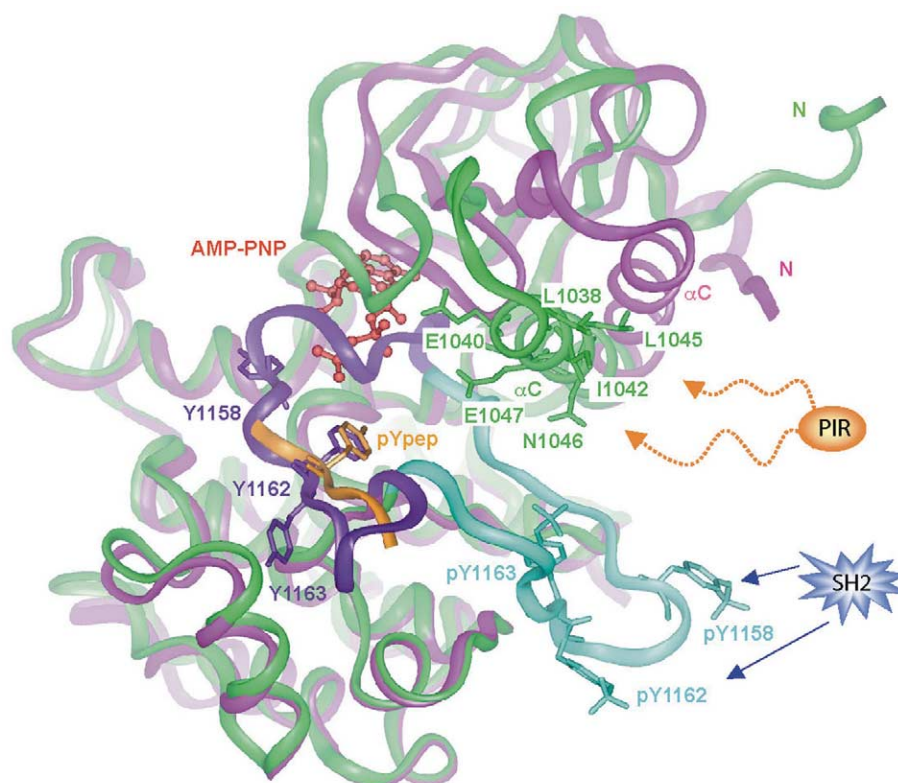


Fig. 4. A proposed model for the interaction of PIR-SH2 Grb14 with IR. Superposition on all C α of the unphosphorylated insulin receptor kinase domain (PDB code: 1IRK) colored pink, with the triphosphorylated IRK (PDB code: 1IR3) colored green. The activation loops of IRK and IR3 are colored purple and light blue, respectively. The backbone of the peptide substrate is brown and AMP-PNP is red. The phosphotyrosines, the αC residues of IR3 and the most unmasked amino acids (L1038, I1042 and L1045) upon rearrangement of the IR3P activation loop are represented. The arrows (blue/orange) indicate the plausible interaction of PIR and SH2 domains of Grb14 with IR.

undergoes a major conformational change of 30 Å away from its original position allowing access to the ATP and to the substrate binding sites. pY1162 was shown to be the key phosphotyrosine in stabilizing the kinase loop conformation, followed by pY1163 and pY1158 [39]. Up to now, it is unclear if the interaction of PIR-SH2 with IR is mediated by the sequence of the loop, a specific structure of this loop, or by interactions with the residues unmasked by the loop rearrangement. Peptide competition experiments have shown that PIR-IR binding is not a phosphotyrosine-mediated interaction [10], which abolishes the first hypothesis.

From crystallographic studies of IR performed by Hubbard [39], it has been observed that the rearrangement of the IR kinase loop upon autophosphorylation reorients the C- and N-terminal lobes of the kinase. This movement allows residues of α C to become solvent-exposed and therefore involved in protein–protein interactions. Consequently it can be hypothesized that because of the suggested extended form of PIR domain, this one could take place in the cleft between the N- and C-terminal lobes of the kinase and could interact with the solvent-exposed residues of α C (Fig. 4). On this suggested model of PIR-IR binding, the access of ATP and of the substrate to their respective sites would not be blocked, which is consistent with the fact that Grb14 behaves as a non-competitive inhibitor. Furthermore, the SH2 domain could stabilize the PIR-IR binding by interacting with the phosphorylated regulatory kinase loop. Our oocyte experiments showed that the inhibitory activity of PIR is six times less efficient than that of PIR-SH2. This is in good agreement with the reported Grb14 interaction with IR [8]. The fact that PIR alone interacts less efficiently with IR than PIR-SH2 suggests a role for the SH2 domain in the stabilization of PIR binding. This could explain the relative importance of the two domains PIR and SH2 of the Grb7/10/14 proteins in the interaction with IR. It has been reported that the SH2 domain is responsible for the binding of Grb7 to the IR, whereas PIR and SH2 are equally important in the Grb10/IR interaction, and PIR is the main binding domain in the IR-Grb14 interaction.

The SH2 domain of Grb7 displays the same consensus binding site as Grb2 with the presence of an asparagine at the +2 position following the phosphotyrosine [40,41]. In addition the SH2 recognition sequence 'pYpY', which corresponds to residues 1162–1163 of the IR activation loop, has only been reported for Grb2 [42]. This could explain why the SH2 of Grb7 appears to bind with higher affinity with the phosphorylated IR than the SH2 of Grb10/14. For the two other Grbs, the SH2 interaction can suffer a mismatch minimizing their action as in the Src structure [43], or they can bind preferentially to pY1158 instead of pY1162/pY1163. This model is supported by the recent study of the crystal structure of Grb10 γ [44] SH2 domain that appears to be a dimer. It has been proposed that the SH2 dimer binds to the activation loops of the two tyrosine kinase domains of the IR β subunits with pY1158 in the canonical phosphotyrosine binding pocket of each SH2 domain.

Further studies are needed to map the region involved in the interaction with IR, and in the interaction with ZZ zinc finger domain of the adapter protein ZIP. Identification of the specific targets of PIR will be a necessary step to perform structural studies, and to provide more information in the signaling specificity of the different members of the Grb7 family of proteins.

Acknowledgements: We thank F. Dardel for its helpful comments on the manuscript. This work was supported by ACI of the French Ministry of Research (MENRT), and by a grant from the 'Association pour la Recherche sur le Cancer' (grant n°5217 to A.F.B.). K.M. is the recipient of a fellowship from the French Ministry of Research (MENRT) and from the 'Ligue Nationale Contre le Cancer'.

References

- [1] Daly, R.J. (1998) *Cell Signal* 10, 613–618.
- [2] Han, D.C., Shen, T.L. and Guan, J.L. (2001) *Oncogene* 20, 6315–6321.
- [3] Tanaka, S., Mori, M., Akiyoshi, T., Tanaka, Y., Mafune, K., Wands, J.R. and Sugimachi, K. (1997) *Cancer Res.* 57, 28–31.
- [4] Tanaka, S., Sugimachi, K., Kawaguchi, H., Saeki, H., Ohno, S. and Wands, J.R. (2000) *J. Cell Physiol.* 183, 411–415.
- [5] Han, D.C. and Guan, J.L. (1999) *J. Biol. Chem.* 274, 24425–24430.
- [6] Han, D.C., Shen, T.L. and Guan, J.L. (2000) *J. Biol. Chem.* 275, 28911–28917.
- [7] Nantel, A., Mohammad-Ali, K., Sherk, J., Posner, B.I. and Thomas, D.Y. (1998) *J. Biol. Chem.* 273, 10475–10484.
- [8] Kasus-Jacobi, A., Perdureau, D., Auzan, C., Clauser, E., Van Obberghen, E., Mauvais-Jarvis, F., Girard, J. and Burnol, A.F. (1998) *J. Biol. Chem.* 273, 26026–26035.
- [9] Hemming, R., Agatep, R., Badiani, K., Wyant, K., Arthur, G., Gietz, R.D. and Triggs-Raine, B. (2001) *Biochem. Cell Biol.* 79, 21–32.
- [10] Stein, E.G., Gustafson, T.A. and Hubbard, S.R. (2001) *FEBS Lett.* 493, 106–111.
- [11] Bereziat, V., Kasus-Jacobi, A., Perdureau, D., Cariou, B., Girard, J. and Burnol, A.F. (2002) *J. Biol. Chem.* 277, 4845–4852.
- [12] He, W., Rose, D.W., Olefsky, J.M. and Gustafson, T.A. (1998) *J. Biol. Chem.* 273, 6860–6867.
- [13] Kasus-Jacobi, A., Bereziat, V., Perdureau, D., Girard, J. and Burnol, A.F. (2000) *Oncogene* 19, 2052–2059.
- [14] Cariou, B., Perdureau, D., Cailliau, K., Browaeys-Poly, E., Bereziat, V., Vasseur-Cognet, M., Girard, J. and Burnol, A.F. (2002) *Mol. Cell. Biol.* 22, 6959–6970.
- [15] Hansen, H., Svensson, U., Zhu, J., Laviola, L., Giorgino, F., Wolf, G., Smith, R.J. and Riedel, H. (1996) *J. Biol. Chem.* 271, 8882–8886.
- [16] Frantz, J.D., Giorgetti-Peraldi, S., Ottinger, E.A. and Shoelson, S.E. (1997) *J. Biol. Chem.* 272, 2659–2667.
- [17] Bernstein, F.C., Koetzle, T.F., Williams, G.J., Meyer Jr., E.F., Brice, M.D., Rodgers, J.R., Kennard, O., Shimanouchi, T. and Tasumi, M. (1977) *J. Mol. Biol.* 112, 535–542.
- [18] Bax, A., Clore, G.M., Driscoll, P.C., Gronenborn, A.M., Ikura, M. and Kay, L.E. (1990) *J. Magn. Reson.* 29, 8172.
- [19] Schleucher, J., Schwendinger, M., Sattler, M., Schmidt, P., Schedletzky, O., Glaser, S.J., Sorensen, W. and Griesinger, C. (1994) *J. Biomol. NMR* 4, 301–306.
- [20] Sklenar, V., Piatto, M., Leppik, R. and Saudek, V. (1993) *J. Magn. Reson. Ser. A* 102, 241–245.
- [21] Palmer, A.G., Cavanagh, J., Wright, P.E. and Rance, M. (1991) *J. Magn. Reson.* 93, 151–170.
- [22] Kay, L.E., Torchia, D.A. and Bax, A. (1989) *Biochemistry* 23, 8972–8979.
- [23] Muchmore, D.C., McIntosh, L.P., Russell, C.B., Anderson, D.E. and Dahlquist, F.W. (1989) *Methods Enzymol.* 177, 44–73.
- [24] Lemesle-Varloot, L., Henrissat, B., Gaboriaud, C., Bissery, V., Morgat, A. and Mornon, J.P. (1990) *Biochimie* 72, 555–574.
- [25] Gopal, B., Papavinasasundaram, K.G., Dodson, G., Colston, M.J., Major, S.A. and Lane, A.N. (2001) *Biochemistry* 40, 920–928.
- [26] Yao, J., Dyson, H.J. and Wright, P.E. (1997) *FEBS Lett.* 419, 285–289.
- [27] Yao, J., Chung, J., Eliezer, D., Wright, P.E. and Dyson, H.J. (2001) *Biochemistry* 40, 3561–3571.
- [28] Renner, C., Schleicher, M., Moroder, L. and Holak, T.A. (2002) *J. Biomol. NMR* 1, 23–33.
- [29] Muslin, A.J., Klippel, A. and Williams, L.T. (1993) *Mol. Cell. Biol.* 13, 6661–6666.
- [30] Katzav, S., Packham, G., Sutherland, M., Aroca, P., Santos, E. and Cleveland, J.L. (1995) *Oncogene* 11, 1079–1088.

- [31] Yim, D.L., Opresko, L.K., Wiley, H.S. and Nuccitelli, R. (1994) *Dev. Biol.* 162, 41–55.
- [32] Tompa, P. (2002) *Trends Biochem. Sci.* 27, 527.
- [33] Dunker, A.K., Lawson, J.D., Brown, C.J., Williams, R.M., Romero, P., Oh, J.S., Oldfield, C.J., Campen, A.M., Ratliff, C.M., Hipps, K.W., Ausio, J., Nissen, M.S., Reeves, R., Kang, C., Kissinger, C.R., Bailey, R.W., Griswold, M.D., Chiu, W., Garner, E.C. and Obradovic, Z. (2001) *J. Mol. Graph. Model* 19, 26–59.
- [34] Uversky, V.N. (2002) *Eur. J. Biochem.* 269, 2–12.
- [35] Uversky, V.N. (2002) *Protein Sci.* 11, 739–756.
- [36] Wright, P.E. and Dyson, H.J. (1999) *J. Mol. Biol.* 293, 321–331.
- [37] Dyson, H.J. and Wright, P.E. (2002) *Curr. Opin. Struct. Biol.* 12, 54–60.
- [38] Hubbard, S.R., Wei, L., Ellis, L. and Hendrickson, W.A. (1994) *Nature* 372, 746–754.
- [39] Hubbard, S.R. (1997) *EMBO J.* 16, 5572–5581.
- [40] Jones, N., Master, Z., Jones, J., Bouchard, D., Gunji, Y., Sasaki, H., Daly, R., Alitalo, K. and Dumont, D.J. (1999) *J. Biol. Chem.* 274, 30896–30905.
- [41] Pero, S.C., Oligino, L., Daly, R.J., Soden, A.L., Liu, C., Roller, P.P., Li, P. and Krag, D.N. (2002) *J. Biol. Chem.* 277, 11918–11926.
- [42] Nioche, P., Liu, W.Q., Broutin, I., Charbonnier, F., Latreille, M.T., Vidal, M., Roques, B., Garbay, C. and Ducruix, A. (2002) *J. Mol. Biol.* 315, 1167–1177.
- [43] Sicheri, F. and Kuriyan, J. (1997) *Curr. Opin. Struct. Biol.* 7, 777–785.
- [44] Stein, E.G., Ghirlando, R. and Hubbard, S.R. (2003) *J. Biol. Chem.* 278, 13257–13264.